Radiation Measurements 176 (2024) 107217

Contents lists available at ScienceDirect

Radiation Measurements

journal homepage: www.elsevier.com/locate/radmeas

Development of $CaSO_4$:RE,Li (RE = Tm, Eu, Tb) composites for thermally or optically stimulated luminescence dosimetry

Danilo O. Junot [a,*], Diego C. Galeano [b], Anderson M.B. Silva [c], Divanizia N. Souza [d], Linda V.E. Caldas [c]

[a] Instituto de Física Armando Dias Tavares, Universidade do Estado do Rio de Janeiro UERJ, Rio de Janeiro, RJ, Brazil
[b] Hospital Universitário Júlio Muller, Universidade Federal do Mato Grosso UFMT (HUJM-UFMT/EBSERH), Cuiabá, MT, Brazil
[c] Instituto de Pesquisas Energéticas e Nucleares/Comissão Nacional de Energia Nuclear IPEN/CNEN, São Paulo, SP, Brazil
[d] Departamento de Física, Universidade Federal de Sergipe UFS, São Cristóvão, SE, Brazil

ARTICLE INFO

Keywords:
$CaSO_4$
Synthesis methods
Radiation dosimetry
Thermoluminescence
Optically stimulated luminescence

ABSTRACT

This work proposed the development of $CaSO_4$:Tm,Li, $CaSO_4$:Tb,Li and $CaSO_4$:Eu,Li composites for application in radiation dosimetry, using luminescent techniques such as thermoluminescence (TL) and optically stimulated luminescence (OSL). The $CaSO_4$ crystals were produced by the adapted slow evaporation route and characterized using X-ray diffraction (XRD), TL and OSL techniques. XRD analyses showed that the doped $CaSO_4$ samples presented a single phase. The $CaSO_4$:Eu,Li composites showed TL signals with peaks around 145 °C and 180 °C. The $CaSO_4$:Tb,Li and $CaSO_4$:Tm,Li composites showed TL signals with peaks centered at 165 °C and 275 °C. For the $CaSO_4$:Tb and $CaSO_4$:Tm samples, the addition of lithium as co-dopant resulted into a significant increase (2x) in the total TL signal of the samples. The $CaSO_4$:Tm,Li samples presented a very intense OSL signal, about 80x greater than the signal of the other samples produced. This allows the applicability of TL/OSL detectors even more sensitives. The TL emission spectra of the samples showed typical emissions of Eu^{2+} ions (280 nm), Eu^{3+} (614 nm), Tb^{3+} (544 nm) and Tm^{3+} (455 nm). No emission corresponding to lithium was identified. All the samples produced showed linearity in the dose range used and good reproducibility, with variations below 10%. The $CaSO_4$:Tm,Li samples showed the lowest limit of detection and fading. The evaluated dosimetric characteristics denote that these developed composites have potential application as TL/OSL detectors.

1. Introduction

Luminescent techniques such as thermoluminescence (TL) and optically stimulated luminescence (OSL) are quite useful for estimating the dose of ionizing radiation absorbed in various types of monitoring. The fact that OSL does not require a heating system, which consumes a lot of energy and time, and still does not destroy the sample signal, ensures advantages to OSL in the competition among techniques, although TL has been established for decades.

Luminescent dosimeters have extensive use, mainly due to the possibility of reuse, high sensitivity, easy production, great commercial viability, and availability in small sizes, which allows dose monitoring in difficult geometries. These characteristics make TL/OSL dosimeters widely used in in vivo dosimetry, in the planning and execution of various radiotherapeutic procedures (Souza et al., 2008). During use, these dosimeters are usually protected in cases made of materials with low attenuation coefficient for ionizing radiation and high light attenuation, so that it does not influence the TL/OSL signal (Campos, 1998; Lakshmanan, 1999).

$CaSO_4$ is one of the most sensitive thermoluminescent materials ever evaluated, and studies have reported that, when doped with rare earth elements and silver nanoparticles, this material presents characteristics that make it promising to be applied as TL/OSL dosimeter (Junot et al., 2019, 2020; Silva et al., 2020). Several researchers (Kulkarni et al., 2014; Kearfott et al., 2015; Guckan et al., 2017; Junot et al., 2014, 2019; Silva et al., 2021) have systematically studied the TL/OSL response of $CaSO_4$ phosphors doped with europium, terbium, and thulium, but there are no reports in the literature regarding the use of $CaSO_4$:RE,Li (RE = Tm,Eu,Tb) in this type of dosimetry.

Thus, this work proposed the development of composites of $CaSO_4$: Tm,Li, $CaSO_4$:Tb,Li, and $CaSO_4$:Eu,Li for application in radiation dosimetry, using luminescent techniques such as thermoluminescence

* Corresponding author.
E-mail address: dan.junot@gmail.com (D.O. Junot).

https://doi.org/10.1016/j.radmeas.2024.107217
Received 28 February 2024; Received in revised form 19 June 2024; Accepted 21 June 2024
Available online 22 June 2024

(TL) and optically stimulated luminescence (OSL). The development and use of new dosimetric materials for investigations in quality control in medicine, personal and environmental monitoring, and in industrial processes employing ionizing radiation are of utmost importance to this area of knowledge, in order to provide sensitive and low-cost detectors.

2. Experimental procedure

2.1. Production of the samples

The production of the composites used in this work was carried out through two stages: growth of $CaSO_4$ crystals and production of the pellets, which are the dosimeters to be employed.

The $CaSO_4$ crystals were produced by an adaptation of the slow evaporation route. This route is based on the mixture of calcium carbonate ($CaCO_3$ - Merck - 99% purity), sulfuric acid (H_2SO_4 - Dinâmica - 95% purity), and the dopant oxide in mol% proportions of the mass of $CaCO_3$. In the synthesis of $CaSO_4$:Tm,Li, thulium oxide (Tm2O3 - Sigma-Aldrich - 99.9% purity) and lithium carbonate (Li_2CO_3 - Sigma-Aldrich - 99% purity) were used, both at a proportion of 0.1 mol%. The synthesis of $CaSO_4$:Eu,Li and $CaSO_4$:Tb,Li samples was done in the same way, using europium oxide (Eu_2O_3 - Sigma-Aldrich - 99.9% purity) and terbium oxide (Tb_4O_7 - Sigma-Aldrich - 99.9% purity), respectively. To obtain the crystals, the $CaSO_4$+H_2SO_4+H_2O + dopants solution, resulting from the mixture, was deposited in a beaker and remained on a magnetic stirrer at 120 °C until complete homogenization and evaporation of water. Subsequently, the solution was introduced into a volumetric flask on a heating mantle at 375 °C until all the acid evaporated (approximately 24 h). Acid vapors were condensed and collected in an Erlenmeyer flask at the condenser outlet. This is an important step added to the route, as the condensed acid can be reused in new $CaSO_4$ crystal growths. Possible uncondensed vapors were stored in wash bottles containing 250 mL of sodium hydroxide solution for neutralization. The crystal growth was carried out in a sealed vacuum system. The $CaSO_4$ powder adhered to the wall of the volumetric flask after acid evaporation was then transferred to a beaker and underwent a series of washes with hot water (100 °C) and cold water (room temperature, approximately 25 °C), alternately, until the pH of the samples was around 6.

With crystals ranging from 75 μm to 150 μm in grain size, pellets were made by adding 50% by mass of polytetrafluoroethylene (Teflon) to improve the material's resistance. The produced pellets were subjected to a uniaxial pressing of 2 tons and sintered at 400 °C for 1 h, since the melting point of Teflon is around 400 °C (D'Amorim et al.). After sintering, the pellets had approximately 1 mm thickness and 6 mm diameter, and weighed around 40 mg.

2.2. Structural characterization

In order to perform the structural characterization of the produced crystals, X-ray diffraction (XRD) technique was used, which aims primarily to identify parameters of the crystalline structure, including the phases present in the samples. XRD measurements were carried out on a Rigaku diffractometer (RINT, 2000/PC), using Cu Kα radiation, with the X-ray tube operating at 40 kV and 30 mA, in continuous scanning mode from 20° to 80°, with steps of 0.05°/min.

2.3. Dosimetric characterization

The TL and OSL readings used for the dosimetric characterization of the materials were performed on the Risø TL/OSL Reader, model DA-20, of the Radiation Metrology Laboratory (LMR) of IPEN. This reader consists of a heating system, blue and infrared Light Emitting Diodes (LEDs), a photomultiplier, optical filters, a carousel with support for 48 samples, and sources of $^{90}Sr/^{90}Y$ (beta emitter) and ^{241}Am (alpha emitter) coupled. TL analyses were performed using a heating rate of 10 °C/s, up to a maximum temperature of 400 °C. Although this heating rate is commonly used in dosimetry, heating rates of 5 °C/s or less are typically employed for TL emission analysis of materials. However, lower heating rates require longer acquisition times, which were not feasible in this work, posing limitations for comparison of results with other studies available in the literature. Blue LEDs with an emission wavelength of 470 nm and operating in continuous-wave mode were employed for sample excitation in OSL measurements. In all analyses, the Hoya U-340 filter was used, with a transmission band between 250 nm and 390 nm.

All samples were irradiated with the $^{90}Sr/^{90}Y$ beta source coupled with the TL/OSL Riso reader, at a rate of 79 mGy/s. The doses applied ranged from 81 mGy to 50 Gy.

TL emission spectra were evaluated during the heating of the samples up to 400 °C at a rate of 10 °C/s. For the measurements, the samples were irradiated with a dose of 50 Gy, and a high-resolution spectrometer from Ocean Optics was attached in place of the photomultiplier in the Risø TL/OSL reader.

3. Results and discussions

3.1. Structural characterization

Fig. 1 presents the XRD results for the prepared samples, in powder form, after calcination. The diffraction patterns obtained for all samples showed diffraction peaks and relative intensities corresponding to the anhydrite structure (JCPSD 01-072-0916). Thus, it can be observed that the doped $CaSO_4$ samples exhibited only a single phase, as expected, since the technique does not allow the observation of dopants at concentrations lower than 5%. These results confirm that the samples are composed of $CaSO_4$ crystals with orthorhombic symmetry and Amma space group, consistent with the results reported by Junot et al. (2014) for $CaSO_4$:Eu samples, Junot et al. (2019) for $CaSO_4$:Tm samples, and Silva et al. (2020) for $CaSO_4$:Tb samples.

3.2. Dosimetric characterization

Fig. 2 shows the characteristic TL glow curves of the $CaSO_4$:Eu, $CaSO_4$:Eu,Li, $CaSO_4$:Tb, $CaSO_4$:Tb,Li, $CaSO_4$:Tm, and $CaSO_4$:Tm,Li composites after irradiation with 300 mGy of beta radiation from the $^{90}Sr/^{90}Y$ source. The heating rate used in the readings was 10 °C/s. It can be observed that the addition of lithium to the doped composites does not alter the emission temperature of the TL peaks of the samples;

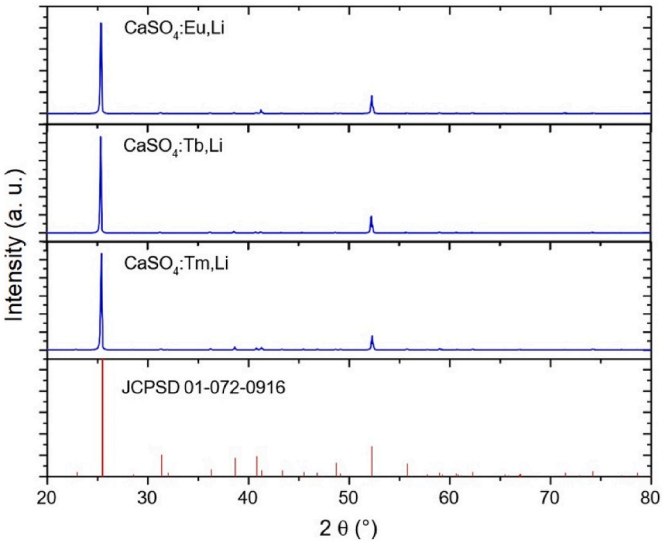

Fig. 1. X-ray diffractograms of crystalline samples of $CaSO_4$*:Eu,Li,* $CaSO_4$*:Tb,Li and* $CaSO_4$*:Tm,Li.*

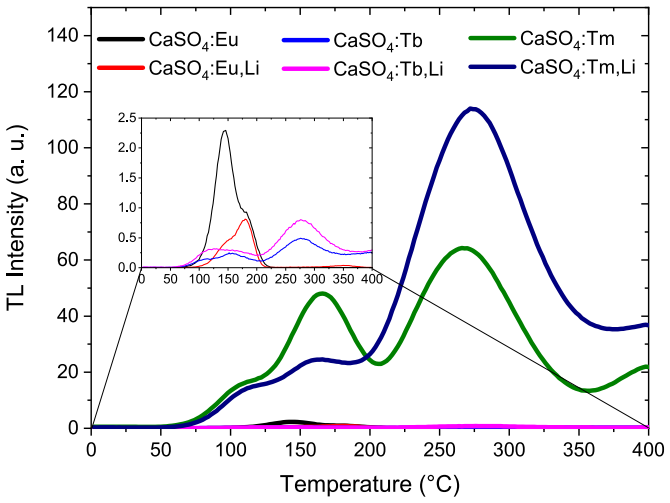

Fig. 2. TL glow curves of $CaSO_4$:*Eu,* $CaSO_4$:*Eu,Li,* $CaSO_4$:*Tb,* $CaSO_4$:*Tb,Li,* $CaSO_4$:*Tm and* $CaSO_4$:*Tm,Li samples after irradiation with* 300 mGy ($^{90}Sr/^{90}Y$).

however, it strongly affects their emission intensities. The $CaSO_4$:Eu and $CaSO_4$:Eu,Li composites exhibited TL signals between 100 °C and 200 °C, with peaks around 145 °C and 180 °C. It can be observed that the addition of lithium drastically reduces the intensity of the peak around 145 °C while not altering the intensity of the peak around 180 °C, resulting in a decrease in the total TL signal of the sample. In contrast, for the $CaSO_4$:Tb and $CaSO_4$:Tm samples, the addition of lithium resulted in a significant increase in the total TL signal of the samples, as the intensity of the peak around 275 °C of both samples practically doubled. This result represents an important advantage of lithium addition in these samples. As expected, samples doped with thulium exhibited considerably more intense emission, about 40 times greater, than samples doped with europium or terbium. Junot et al. (2014, 2019) and Silva et al. (2020) reported similar TL emission curves for $CaSO_4$:Eu, $CaSO_4$:Tm, and $CaSO_4$:Tb samples, respectively, with only differences in intensity.

It is necessary to investigate, through optical characterization, the mechanisms involved in suppressing the TL intensity of the peak around 145 °C of the $CaSO_4$:Eu,Li samples. However, the considerable increase in intensity resulting from the insertion of lithium into the $CaSO_4$:Tb and $CaSO_4$:Tm samples leads us to the hypothesis that lithium probably acts as a low-efficiency luminescent and recombination center but transfers its energy to the nearby RE^{3+}, thereby increasing luminescence. Another possibility is that lithium is acting as a charge compensator and enabling the incorporation of RE^{3+} ions into the matrix. To achieve charge compensation in $CaSO_4$:RE^{3+}, the insertion of the ion leads to the creation of calcium vacancies (2 $RE^{3+} \rightarrow Ca^{2+}$ vacancy). The addition of lithium reduces the vacancies ($Li^+ + RE^{3+} \rightarrow 2\ Ca^{2+}$), allowing more RE^{3+} ions to be incorporated into the matrix.

Assessing the dosimetric applicability of the samples with the results at hand, it can be stated that the addition of lithium to $CaSO_4$:Tm samples presents significant advantages. It is well known that a good dosimetric peak should be a single peak at a temperature of 200–300 °C (McKeever et al., 1995). In this case, it is at a low enough temperature to minimize the time and energy spent in the reading process, as well as high enough to minimize fading issues. $CaSO_4$:Tm,Li exhibits a clear sensitivity advantage and displays a main peak at 275 °C, easily considered a good dosimetric peak. However, additional analyses using Tm-Tstop techniques are necessary to verify if this is a single peak or is composed of an overlap of multiple peaks over a wide range of temperatures. The complexity of TL curves, especially those composed of many peaks, has been reported by some researchers (Nunes and Campos, 2008; Souza et al., 2015; Doull et al., 2014; Junot et al., 2019).

The TL emission characteristics of the produced samples were analyzed using the (Tm-Tstop) technique, involving the controlled heating of each sample to a designated temperature (Tstop), followed by the assessment of the average temperature corresponding to the lowest temperature peak observed (Tm). Initially, the samples were irradiated with a dose of 200 mGy, and partial heating commenced at a starting Tstop temperature of 100 °C. The Tstop pre-heating was conducted at a heating rate of 10 °C/s. Subsequent to this phase, the samples were subjected to cooling, and the complete glow curve was acquired to ascertain the Tm value. The Tstop temperature was systematically adjusted in increments of 10 °C, ultimately reaching a final Tstop temperature of 350 °C for $CaSO_4$:Eu,Li samples and 390 °C for the remaining samples. Analysis of the acquired data facilitated the generation of the "Tm x Tstop" graph, shown in Fig. 3, where the plotted lines delineate the temperatures corresponding to the TL peaks observed in the TL glow curve of the samples. The readings were performed with different samples from the same batch and each data point corresponds to the average of the responses from three samples. Across all samples, a consistent observation of three peaks was noted: $CaSO_4$:Eu,Li exhibited peaks at 180 °C, 206 °C, and 305 °C; $CaSO_4$:Tb,Li displayed peaks at 204 °C, 224 °C, and 355 °C; whereas $CaSO_4$:Tm,Li manifested peaks at 200 °C, 223 °C, and 319 °C.

Fig. 4 presents continuous wave mode (CW) OSL curves with a 40 s integration time for $CaSO_4$:Eu,Li, $CaSO_4$:Tb,Li, and $CaSO_4$:Tm,Li samples. It can be observed that $CaSO_4$:Eu,Li and $CaSO_4$:Tb,Li samples exhibit exponential decay as the optically active traps are emptied, indicating that the traps responsible for OSL decay have a high photoionization cross-section for blue LEDs, meaning the OSL decay of these samples is predominantly governed by a fast decay constant. $CaSO_4$:Tm,Li samples do not exhibit predominance of rapid decay component, so the OSL signal decays slowly and remains stored for a long time. Therefore, it can be inferred that the traps responsible for the luminescent centers that give rise to the TL signal in these samples are not easily stimulated by the blue LED stimulus. However, the samples exhibited a significantly intense OSL signal, about 80 times greater than the signal from the other produced samples. These results are quite similar to the results reported by Junot et al. (2019, 2020) for $CaSO_4$:Eu and $CaSO_4$:Tm co-doped with silver nanoparticles.

The experimental OSL decay curves were fitted with decreasing exponential functions from Eq. (1):

$$I_{OSL} = A_1 e^{-t/\tau_1} + A_2 e^{-t/\tau_2} + A_3 e^{-t/\tau_3} \quad (1)$$

where I_{OSL} is the initial OSL intensity, A_1, A_2, A_3 are constant coefficients and τ_1, τ_2, τ_3 are the decay constants of the respective OSL traps (Barve et al., 2015).

The exponential fitting of the OSL decay curves showed in Fig. 5

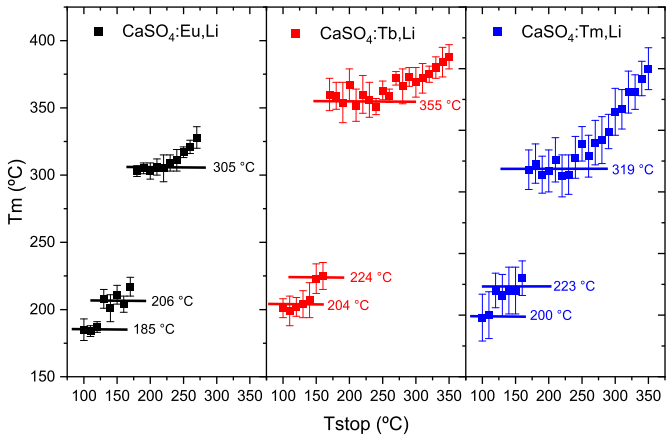

Fig. 3. Tm-Tstop curve of $CaSO_4$:Eu,Li, $CaSO_4$:Tb,Li and $CaSO_4$:Tm,Li samples obtained across a range of pre-heating temperatures (Tstop), under a controlled heating rate of 10 °C/s.

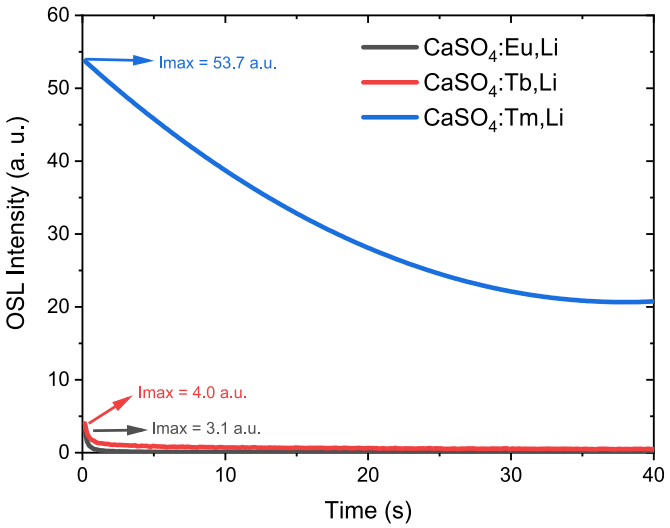

Fig. 4. OSL decay curves of $CaSO_4$:*Eu,Li,* $CaSO_4$:*Tb,Li and* $CaSO_4$:*Tm,Li samples after irradiation with* 1 Gy ($^{90}Sr/^{90}Y$).

yielded constant coefficients and decay constants (lifetimes), as detailed in Table 1. The $CaSO_4$:Eu,Li and $CaSO_4$:Tb,Li samples exhibited higher values for coefficients A_1 compared to A_2 and A_3, thereby corroborating the prevalence of OSL decay curves characterized by fast component. Notably, the contribution of the slow component was minimal, with the highest value of A_3 recorded as only 0.139 for the OSL response of these samples. The adoption of a curve-fitting equation comprising three components was grounded on its capacity to offer a precise depiction of the decay model (Silva et al., 2023). However, for the $CaSO_4$:Tm,Li samples, the decay model incorporating two components was adjudged as furnishing a more accurate estimation. With coefficients A_2 and A_3 approximately at 0.5 and lifetimes of 11.53 (τ_1) and 89.56 (τ_2), it can be inferred that these samples exhibit equal contributions from the medium and slow components, with no presence of a fast component. It was expected since $CaSO_4$:Tm,Li samples showed an overlap of multiple TL peaks over a wide range of temperatures and the OSL decay curve is affected by factors such as trapping at competing traps, simultaneous stimulation from multiple trapping levels, and recombination at multiple recombination centers (Yukihara and McKeever, 2008).

To study the reproducibility of the composites, an extremely important characteristic for TL/OSL dosimeters, 25 pellets of each material were produced, all with a mass of 40 mg. The ratio of the TL response of each dosimeter to the average response of the batch results in the coefficient of homogeneity variance (CV_H) of the dosimeter. To evaluate the TL signal reproducibility, the dosimeters were irradiated with 790 mGy of beta radiation ($^{90}Sr/^{90}Y$) evaluated in the TL reader at

Table 1
OSL parameters obtained from the exponential fit of the curves of $CaSO_4$:Eu,Li, $CaSO_4$:Tb,Li and $CaSO_4$:Tm,Li samples.

SAMPLE	CW-OSL COMPONENT	COEFFICIENT A_I	DECAY CONSTANT T_I (S)
$CaSO_4$:Eu, Li	Fast	1.97 ± 0.03 (A_1)	0.163 ± 0.003 (t_1)
	Medium	0.29 ± 0.02 (A_2)	0.93 ± 0.04 (t_2)
	Slow	0.016 ± 0.001 (A_3)	30.9 ± 2.8 (t_3)
$CaSO_4$:Tb, Li	Fast	1.37 ± 0.03 (A_1)	0.215 ± 0.008 (t_1)
	Medium	0.22 ± 0.01 (A_2)	1.7 ± 0.1 (t_2)
	Slow	0.139 ± 0.004 (A_3)	17.8 ± 0.5 (t_3)
$CaSO_4$:Tm, Li	Fast	–	–
	Medium	0.527 ± 0.009 (A_2)	11.5 ± 0.2 (t_2)
	Slow	0.497 ± 0.009 (A_3)	89.6 ± 3.4 (t_3)

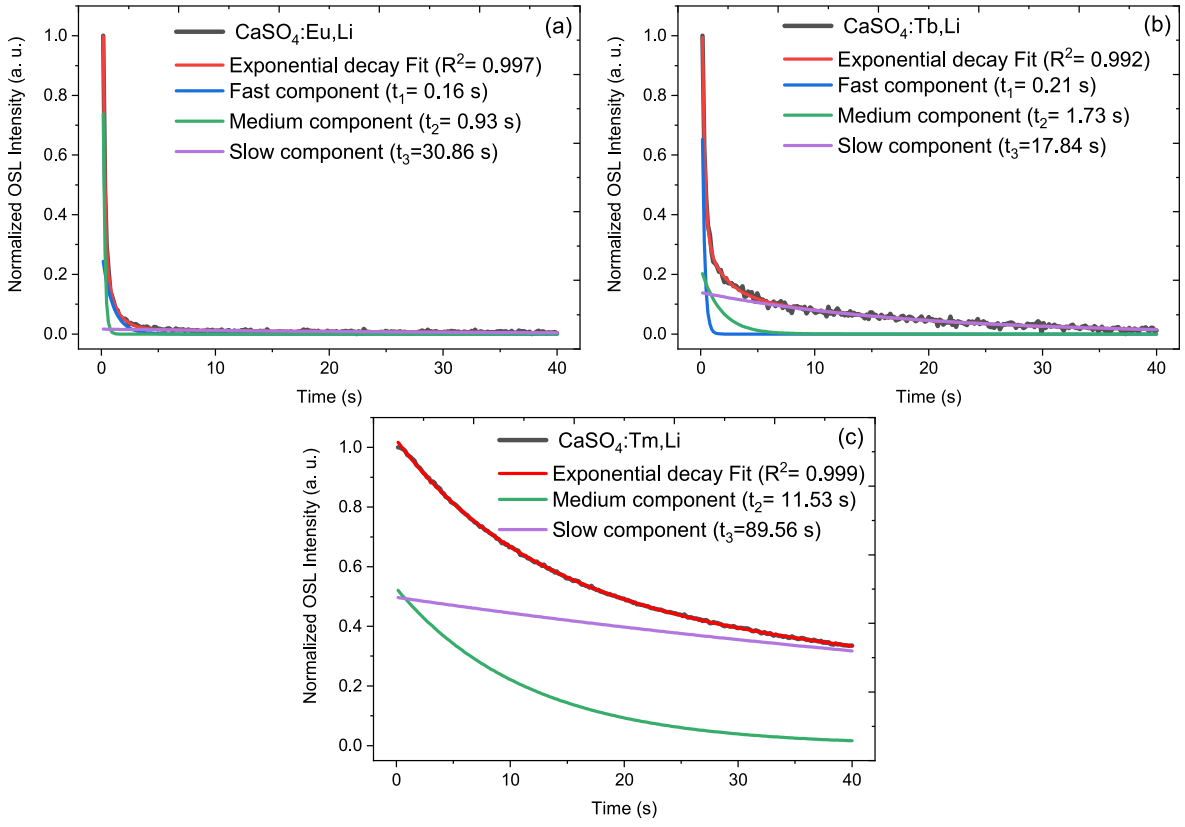

Fig. 5. Experimental and fitted OSL decay curves of $CaSO_4$:Eu,Li (a), $CaSO_4$:Tb,Li (b) and $CaSO_4$:Tm,Li (c) samples.

a heating rate of 10 °C/s, thermally treated, and irradiated again, creating a cycle, which was repeated 5 times. The OSL signal reproducibility was also performed over 5 cycles, but instead of heating, the sample stimulus was light, as described in section 2.3. The TL/OSL responses are the integrated area under the whole corresponding curve. The ratio of the dosimeter's TL response to the average response of the 5 reading cycles results in the coefficient of reproducibility variance (CV_R) of the dosimeter. As observed in Fig. 6a, the TL responses of each material were reproducible, with deviations of only approximately 7%. Fig. 6 also shows the average values of the coefficients of homogeneity and reproducibility variance for each material studied. Fig. 6b shows that the OSL signal of the samples is also reproducible, with deviations of only approximately 3%. All produced samples presented CV_H and CV_R below 9.5% for the TL signal and below 5.4% for the OSL signal.

To assess the linearity of the samples, only 10 dosimeters of each material with CV_H less than 5% relative to the batch were used. Analyzing the calibration curves with log axes on the same scale, as shown in Fig. 7, it can be observed that the TL/OSL response (integrated area under the whole curve) of the composites is linear within the dose range used. The linear correlation coefficients (R^2) for all samples were greater than 0.969. However, for the $CaSO_4$:Tm,Li samples they were greater than 0.998.

To achieve the lowest detectable dose (LDD) of the materials produced, the equation $\mathbf{D_0} = (\mathbf{3}\sigma_{\overline{\mathbf{B}}})\mathbf{f_c}$ proposed by Oberhofer and Scharmann in 1981 was used. In this calculation, $\mathbf{D_0}$ is the LLD, $\sigma_{\overline{B}}$ represents the standard deviation of the measures of non-irradiated dosimeters, commonly known as "background", and $\mathbf{f_c}$ is a calibration factor (the inverse of the slope of the dose-response curve, expressed by Gy/arbitrary units (a.u.)). The estimated LDD values may vary depending on the calculation method and the reader characteristic. Table 2 shows the LDD values obtained for all. As expected, due to their high sensitivity, the $CaSO_4$:Tm,Li samples presented the lowest detection limits (0.3 μGy for TL and 8.6 μGy for OSL).

It is well known that several parameters play a critical role in preserving the stability of trapped charge carriers within the forbidden band gap of a crystal. The decay, or fading, of a TL dosimeter should be minimized, particularly when these materials are stored under optimal conditions such as room temperature and low light exposure. Fig. 8 illustrates the normalized TL/OSL responses of the samples produced post-storage, indicating the decline in the integrated area under the glow curves of the compounds. In this normalization, the TL/OSL response of the samples immediately following irradiation corresponds to a value of 1, with subsequent TL/OSL responses after storage expressed as a percentage relative to this initial response. Notably, all composites exhibit

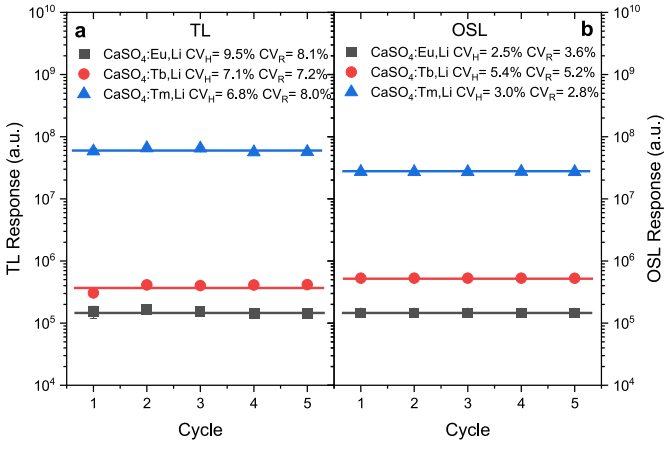

Fig. 6. TL/OSL response (integrated area under the whole curve) of $CaSO_4$:Eu, Li, $CaSO_4$:Tb,Li and $CaSO_4$:Tm,Li samples after each irradiation–reading–annealing cycle. The solid lines represent the average TL response after 5 cycles.

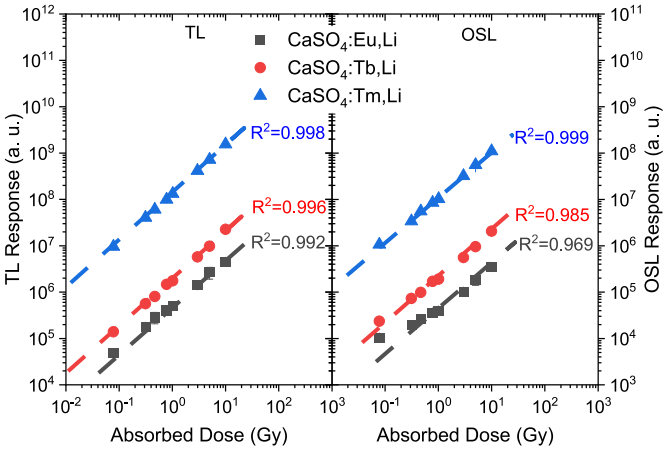

Fig. 7. TL/OSL response (integrated area under the whole curve) of $CaSO_4$:*Eu, Li*, $CaSO_4$:*Tb,Li* and $CaSO_4$:*Tm,Li samples as a function of absorbed dose* ($^{90}Sr/^{90}Y$).

Table 2
Lowest detectable dose (LDD) and parameters used for the LDD calculation of the samples.

Technique	Samples	$\sigma_{\overline{B}}$ (a.u.)	f_c (Gy/a.u.)	LDD (Gy)
TL	$CaSO_4$:Eu,Li	161	2.0×10^{-7}	9.7×10^{-5}
	$CaSO_4$:Tb,Li	191	5.3×10^{-8}	3.0×10^{-4}
	$CaSO_4$:Tm,Li	152	7.3×10^{-10}	3.3×10^{-7}
OSL	$CaSO_4$:Eu,Li	153	2.7×10^{-6}	1.2×10^{-3}
	$CaSO_4$:Tb,Li	278	4.8×10^{-7}	4.0×10^{-4}
	$CaSO_4$:Tm,Li	318	9.0×10^{-9}	8.6×10^{-6}

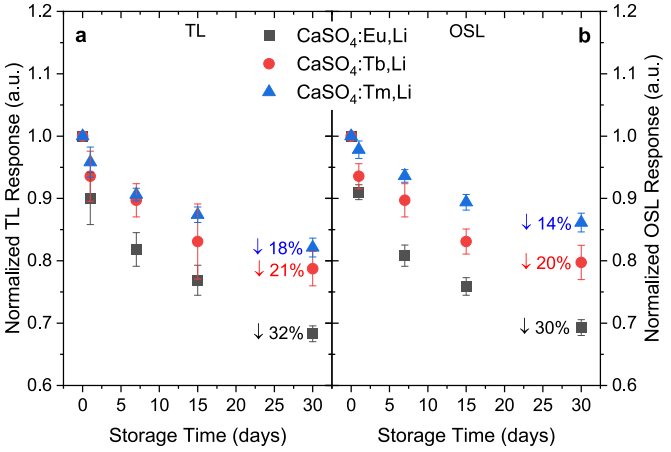

Fig. 8. Normalized TL/OSL response (integrated area under the whole curve) of $CaSO_4$:*Eu,Li,* $CaSO_4$:*Tb,Li and* $CaSO_4$:*Tm,Li samples after different storage times.*

similar TL/OSL signal fading behaviours. Specifically, $CaSO_4$:Eu,Li samples experienced a decrease in TL signal intensity of 10% after one day, 18% after 7 days, 23% after 15 days, and 32% after one month. $CaSO_4$:Tb,Li samples presented a decrease in TL signal intensity of 6% after one day, 10% after 7 days, 17% after 15 days, and 21% after one month. In contrast, $CaSO_4$:Tm,Li samples demonstrated more favorable outcomes, with a reduction in TL signal intensity of approximately 13% over 15 days and 18% after one month. The OSL signal of the $CaSO_4$:Eu, Li samples decays 24% after 15 days, and 30% after one month. $CaSO_4$: Tb,Li samples showed a OSL signal decay of 16% after 15 days, and 20% after one month while $CaSO_4$:Tm,Li samples presented a lower reduction in OSL signal: 11% over 15 days and 14% after one month.

The significant fading observed in the TL signal of the samples can be

mitigated by assessing the fading of the dosimeters following an adequate pre-heating process or by taking into account the higher intensity of the dosimetric peak. Peaks occurring at lower temperatures typically demonstrate reduced stability and decay more rapidly compared to peaks at higher temperatures associated with deeper traps. Fig. 9 presents the decay of the dosimetric peak intensity of the composites after storage. For the $CaSO_4$:Eu,Li samples, the dosimetric peak is centered at 180 °C. For both $CaSO_4$:Tb,Li and $CaSO_4$:Tm,Li samples, the dosimetric peak is centered at 275 °C. Considering the dosimetric peak intensity decay, the fading of the samples is 26%, 16%, and 10% over 30 days for Eu, Tb, and Tm-doped samples, respectively.

The dissimilarity in TL and OSL fading suggests that the recombination centers responsible for OSL emission differ from those responsible for TL emission. Furthermore, given that the fading of the OSL response in these samples mirrors the fading of the TL response rather than the intensity fading of the dosimetric TL peak, it suggests that the OSL emission is primarily attributed to shallow traps.

3.3. TL emission spectra

In order to verify the recombination centers responsible for the TL emissions of the produced samples, TL emission spectra were evaluated. The emission spectrum of the $CaSO_4$:Eu,Li samples is shown in Fig. 10. The emissions corresponding to Eu^{2+} ions can be observed, with emission at 380 nm, and those corresponding to Eu^{3+} ions, with emissions at 590 nm ($^5D_0 \rightarrow {}^7F_1$), 614 nm ($^5D_0 \rightarrow {}^7F_2$), and 695 nm ($^5D_0 \rightarrow {}^7F_4$), indicating that both ions were incorporated into the $CaSO_4$ matrix. The emission in the infrared region (900–1000 nm) over 350 °C is related to the incandescence of the heating plate. The $CaSO_4$:Eu,Li samples emitted at the same wavelength reported by Junot et al. (2020) for the $CaSO_4$:Eu TL emission. It was not possible to observe emissions characteristic of lithium, which can strengthen the hypothesis that lithium acts as a low-efficiency luminescent and recombination center, but transfers its energy to the nearby RE^{3+}, thus increasing luminescence. Since the energy transfer only occurs to the nearby RE^{3+} ion, the addition of lithium in the $CaSO_4$:Eu matrix enhances the Eu^{3+} ion emission and reduces the Eu^{2+} ion emission. However, the Li^+ ions may induce charge compensation and enhancing the insertion of Eu^{3+} ions instead of Eu^{2+} ions, as discussed in section 3.2. This phenomenon was not observed in $CaSO_4$,Eu,Ag samples, where the insertion of silver ions favored the luminescent emission of the Eu^{2+} ion (Junot et al., 2020). It is worth noting that in the TL glow curve reported in Fig. 2, emissions

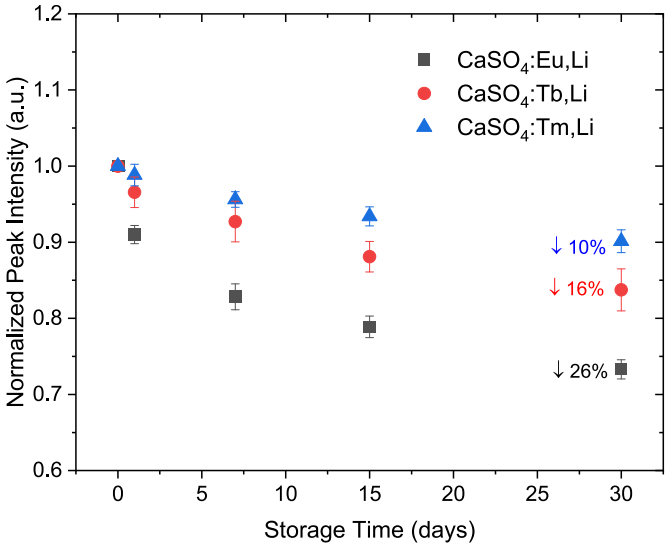

Fig. 9. Normalized dosimetric peak intensity of $CaSO_4$:*Eu,Li,* $CaSO_4$:*Tb,Li and* $CaSO_4$:*Tm,Li samples after different storage times.*

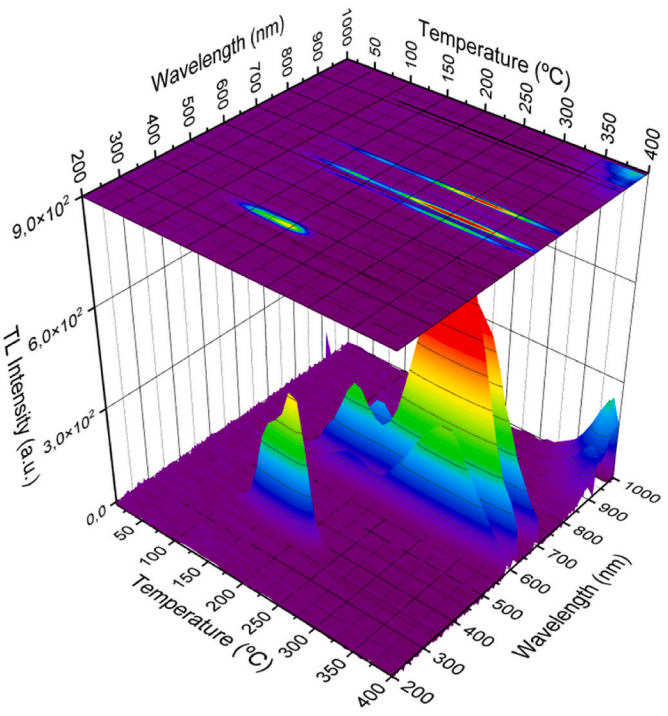

Fig. 10. TL emission spectrum of $CaSO_4$:Eu, Li samples after irradiation with 50 Gy ($^{90}Sr/^{90}Y$).

related to Eu^{3+} ions cannot be observed because the photomultiplier used in TL reading has higher quantum efficiency (or sensitivity) for ultraviolet wavelengths (Eu^{2+}) than for red wavelengths (Eu^{3+}). Additionally, the Hoya U-340 filter, which has transmission only between 250 nm and 390 nm, was used. This could be, at least based on the results obtained, the reason of the decrease in the total TL signal of the $CaSO_4$:Eu,Li samples compared to the $CaSO_4$:Eu samples, as shown in Fig. 2.

The emission spectrum of the $CaSO_4$:Tb,Li samples after being irradiated with a $^{90}Sr/^{90}Y$ source, receiving a dose of 50 Gy, is shown in Fig. 11. The emissions of Tb^{3+} ions can be identified, with the main emission at 544 nm ($^5D_4 \rightarrow {}^7F_5$), and less intense emissions at 412 nm ($^5D_3 \rightarrow {}^7F_5$), 435 nm ($^5D_3 \rightarrow {}^7F_4$), 488 nm ($^5D_4 \rightarrow {}^7F_6$), 586 nm ($^5D_4 \rightarrow {}^7F_4$), and 620 nm ($^5D_4 \rightarrow {}^7F_3$). These are the same emissions reported by Silva et al. (2020) for $CaSO_4$:Tb samples. Once again, it was not possible to observe emissions corresponding to lithium.

Fig. 12 shows the emission spectrum of the $CaSO_4$:Tm,Li samples after being irradiated with a $^{90}Sr/^{90}Y$ source, receiving a dose of 50 Gy. Only emissions from Tm^{3+} ions can be identified, with the main emission at 455 nm ($^1D_2 \rightarrow {}^3F_4$), and less intense emissions at 348 nm ($^1I_6 \rightarrow {}^3F_4$), 355 nm ($^1D_2 \rightarrow {}^3H_6$), 482 nm ($^1G_4 \rightarrow {}^3H_6$), and 788 nm ($^3H_4 \rightarrow {}^3H_6$). These are the same emissions reported by Junot et al. (2019) for $CaSO_4$:Tm samples. Like the spectra of samples doped with europium and terbium, such spectra do not present any emission corresponding to lithium. It can be concluded, therefore, that lithium really acts as a capture center and transfers its energy to nearby RE^{3+}, which increases the intensity of its emission when compared to the emission of the material without lithium.

4. Conclusion

In this paper, the production and structural characterization of the $CaSO_4$:Eu,Li, $CaSO_4$:Tb,Li, and $CaSO_4$:Tm,Li composites were carried out with the purpose of using them as alternative dosimeters to those available in the market, through TL/OSL techniques. The production method and structural characterization indicated that the employed

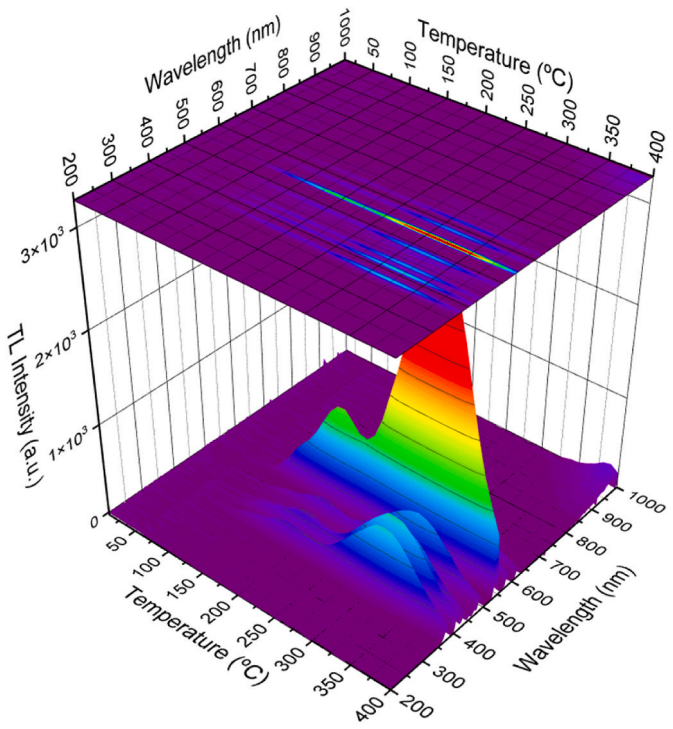

Fig. 11. TL emission spectrum of $CaSO_4$:Tb, Li samples after irradiation with 50 Gy ($^{90}Sr/^{90}Y$).

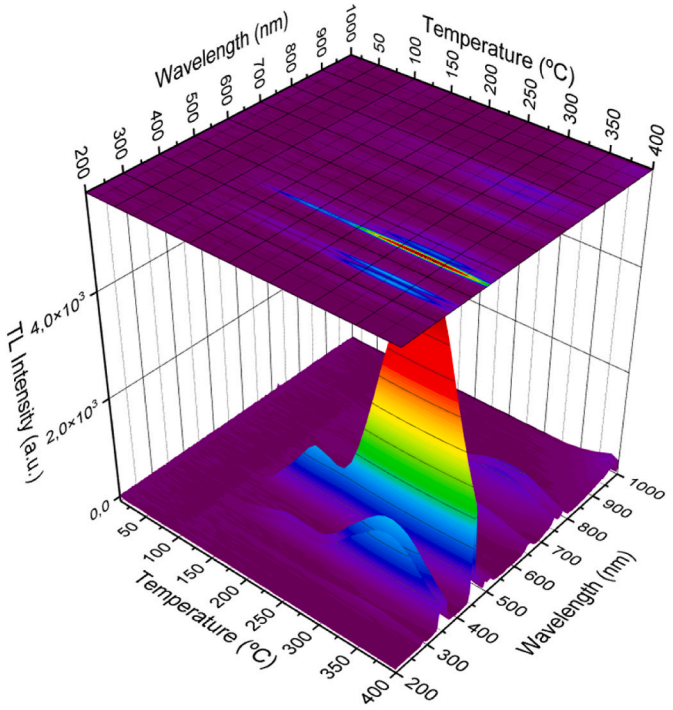

Fig. 12. TL emission spectrum of $CaSO_4$:Tm, Li samples after irradiation with 50 Gy ($^{90}Sr/^{90}Y$).

route is an efficient way to produce $CaSO_4$ composites. The increased luminescent intensity in the $CaSO_4$:Tb,Li and $CaSO_4$:Tm,Li samples represents a significant advantage of adding lithium to these samples. This enhancement results in more sensitive dosimeters capable of detecting lower doses. Since no emission corresponding to lithium was identified in the spectra, it can be presumed that lithium can act as a trapping center and transfer its energy to nearby RE^{3+} ions, or it can act as a charge compensator, enabling the incorporation of more RE^{3+} ions into the matrix. This process thereby increases the emission intensity compared to materials without lithium. OSL results demonstrated a predominance of fast decay component in the $CaSO_4$:Eu,Li and $CaSO_4$:Tb,Li samples exponential signal, and equally contributions of medium and slow decay components for the $CaSO_4$:Tm,Li samples exponential signal. All the samples produced exhibited linearity in the dose range used, good reproducibility, with variations below 10%, and the lowest detectable doses in the order of micrograys. The main drawback of the produced dosimeters is the fading of the luminescence emission, with a signal loss of over 10% after 30 days of storage. Since the $CaSO_4$:Tm,Li samples showed the lowest limit of detection and the best fading, these samples have the highest potential for application as TL/OSL detectors and are suitable for dosimetric procedures in processes involving ionizing radiation where fading is not a critical characteristic.

CRediT authorship contribution statement

Danilo O. Junot: Writing – review & editing, Writing – original draft, Methodology, Investigation, Formal analysis, Data curation, Conceptualization. **Diego C. Galeano:** Validation, Investigation. **Anderson M.B. Silva:** Writing – review & editing, Investigation, Data curation. **Divanizia N. Souza:** Writing – review & editing, Visualization, Investigation. **Linda V.E. Caldas:** Writing – review & editing, Supervision, Funding acquisition.

Declaration of competing interest

The authors declare the following financial interests/personal relationships which may be considered as potential competing interests: Anderson M. B. Silva reports financial support was provided by Brazilian Nuclear Energy Commission. Linda V. E. Caldas reports financial support was provided by National Council for Scientific and Technological Development. Linda V. E. Caldas reports financial support was provided by State of Sao Paulo Research Foundation. If there are other authors, they declare that they have no known competing financial interests or personal relationships that could have appeared to influence the work reported in this paper.

Data availability

Data will be made available on request.

Acknowledgements

The authors thank the Brazilian agencies Comissão Nacional de Energia Nuclear - CNEN (Project 1342.005453/2023–19), Conselho Nacional de Desenvolvimento Científico e Tecnologico - CNPq (Projects: 07493/2021-2, 405536/2023–2, 406761/2022-1, 305142/2021–6 and 406303/2022-3), Fundação de Amparo à Pesquisa do Estado de São Paulo - FAPESP (Project 2018/05982–0) and MultiLab (Multi-User Physics Laboratories) from Federal University of Sergipe for the analysis support.

References

Barve, R.A., Patil, R.R., Moharil, S.V., Bhatt, B.C., Kulkarni, M.S., 2015. Optically stimulated luminescence in Cu+ doped lithium orthophosphate. Phys. B Condens. Matter 458, 117–123. https://doi.org/10.1016/j.physb.2014.11.024.

Campos, L.L., 1998. Termoluminescência de materiais e sua aplicação em dosimetria da radiação. Cerâmica 44, 244–251. https://doi.org/10.1590/S0366-69131998000600007.

D'Amorim, R.A.P.O., Teixeira, M.I., Caldas, L.V.E., Souza, S.O., 2013. Physical, morphological and dosimetric characterization of the Teflon agglutinator to thermoluminescent dosimetry. J. Lumin. 136, 186–190. https://doi.org/10.1016/j.jlumin.2012.11.045.

Doull, B.A., Oliveira, L.C., Wang, D.Y., Milliken, E.D., Yukihara, E.G., 2014. Thermoluminescent properties of lithium borate, magnesium borate and calcium sulfate developed for temperature sensing. J. Lumin. 146, 408–417. https://doi.org/10.1016/j.jlumin.2013.10.022.

Guckan, V., Altunal, V., Nur, N., Depci, T., Ozdemir, A., Kurt, K., Yu, Y., Yegingil, I., Yegingil, Z., 2017. Studying $CaSO_4$:Eu as an OSL phosphor. Nucl. Instrum. Methods Phys. Res. B. 407, 145–154. https://doi.org/10.1016/j.nimb.2017.06.010.

Junot, D.O., Couto, S.M.A., Antonio, P.L., Caldas, L.V.E., Souza, D.N., 2014. Feasibility study of $CaSO_4$:Eu, $CaSO_4$:Eu,Ag and $CaSO_4$:Eu,Ag(NP) as thermoluminescent dosimeters. Radiat. Meas. 71, 99–103. https://doi.org/10.1016/j.radmeas.2014.05.022.

Junot, D.O., Santos, A.G.M., Antonio, P.L., Rezende, M.V.S., Souza, D.N., Caldas, L.V.E., 2019. Dosimetric and optical properties of $CaSO_4$:Tm and $CaSO_4$:Tm,Ag crystals produced by a slow evaporation route. J. Lumin. 210, 58–65. https://doi.org/10.1016/j.jlumin.2019.02.005.

Junot, D.O., Souza, D.N., Caldas, L.V.E., 2020. TL/OSL signal of $CaSO_4$:Eu,Ag samples produced by variations of the slow evaporation route. Radiat. Meas. 135, 106334 https://doi.org/10.1016/j.radmeas.2020.106334.

Kearfott, K.J., West, W.G., Rafique, M., 2015. The optically stimulated luminescence (OSL) properties of LiF:Mg,TI, $Li_2B_4O_7$:Cu, $CaSO_4$:Tm, and CaF_2:Mn thermoluminescent (TL) materials. Appl. Radiat. Isot. 99, 155–161. https://doi.org/10.1016/j.apradiso.2015.03.004.

Kulkarni, M.S., Patilb, R.R., Patleb, A., Rawata, N.S., Ratnaa, P., Bhattc, B.C., Moharil, S. V., 2014. Optically stimulated luminescence from $CaSO_4$:Eu - Preliminary results. Radiat. Meas. 71, 95–99. https://doi.org/10.1016/j.radmeas.2014.02.015.

Lakshmanan, A.R., 1999. Photoluminescence and thermostimulated luminescence processes in rare-earth-doped $CaSO_4$ phosphors. Prog. Mater. Sci. 44, 1–187. https://doi.org/10.1016/S0079-6425(99)00003-1.

McKeever, S.W.S., Moscovitch, M., Townsend, P.D., 1995. Thermoluminescent Dosimetry Materials: Properties and Uses. Kent: Nuclear Technology Publishing.

Nunes, M.G., Campos, L.L., 2008. Study of $CaSO_4$:Dy and LiF:Mg,Ti detectors TL response to electron radiation using a SW Solid Water phantom. Radiat. Meas. 43, 459–462. https://doi.org/10.1016/j.radmeas.2007.11.008.

Oberhofer, M., Scharmann, A., 1981. Applied Thermoluminescence Dosimetry. CRC Press, Ispra.

Silva, A.M.B., Jesus, L.S., Correa, W., Junot, D.O., Caldas, L.V.E., Dantas, N.O., Souza, D. N., Silva, A.C.A., 2023. Luminescence characterization of BioGlass undoped and doped with europium and silver ions. Appl. Radiat. Isot. 201, 110997 https://doi.org/10.1016/j.apradiso.2023.110997.

Silva, A.M.B., Junot, D.O., Caldas, L.V.E., Souza, D.N., 2020. Structural, optical and dosimetric characterization of $CaSO_4$:Tb, $CaSO_4$:Tb, Ag and $CaSO_4$:Tb,Ag(NP). J. Lumin. 224, 117286 https://doi.org/10.1016/j.jlumin.2020.117286.

Silva, A.M.B., Silveira, W.S., Matos, T.S., Junot, D.O., Rezende, M.V.S., Souza, D.N., 2021. Effect of terbium and silver co-doping on the enhancement of photoluminescence in $CaSO_4$ phosphors. Opt. Mater. 111, 110717 https://doi.org/10.1016/j.optmat.2020.110717.

Souza, D.N., Ribeiro, D.R.S., Maia, A.F., Baldochi, S.L., Caldas, L.V.E., 2008. Applicability of pure LiF in dosimetry. Radiat. Meas. 43, 1132–1134. https://doi.org/10.1016/j.radmeas.2007.12.007.

Souza, L.F., Antonio, P.L., Caldas, L.V.E., Souza, D.N., 2015. Neodymium as a magnesium tetraborate matrix dopant and its applicability in dosimetry and as a temperature sensor. Nucl. Instrum. Methods A. 784, 9–13. https://doi.org/10.1016/j.nima.2014.12.030.

Yukihara, E.G., McKeever, S.W.S., 2008. Optically stimulated luminescence (OSL) dosimetry in medicine. Phys. Med. Biol. 53, 351–379.